Constraint Wrench Formulation for Closed-Loop Systems Using Two-Level Recursions

Himanshu Chaudhary
Senior Lecturer
M.L.V. Textile and Engineering College Bhilwara,
Pratap Nagar,
Bhilwara (Rajasthan) 311001, India
e-mail: himanshubhl@rediffmail.com

Subir Kumar Saha
Professor
Department of Mechanical Engineering,
I.I.T. Delhi,
Hauz Khas, New Delhi 110016, India
e-mail: saha@mech.iitd.ernet.in

In order to compute the constraint moments and forces, together referred here as wrenches, in closed-loop mechanical systems, it is necessary to formulate a dynamics problem in a suitable manner so that the wrenches can be computed efficiently. A new constraint wrench formulation for closed-loop systems is presented in this paper using two-level recursions, namely, subsystem level and body level. A subsystem is referred here as the serial- or tree-type branches of a spanning tree obtained by cutting the appropriate joints of the closed loops of the system at hand. For each subsystem, unconstrained Newton–Euler equations of motion are systematically reduced to a minimal set in terms of the Lagrange multipliers representing the constraint wrenches at the cut joints and the driving torques/forces provided by the actuators. The set of unknown Lagrange multipliers and the driving torques/forces associated to all subsystems are solved in a recursive fashion using the concepts of a determinate subsystem. Next, the constraint forces and moments at the uncut joints of each subsystem are calculated recursively from one body to another. Effectiveness of the proposed algorithm is illustrated using a multiloop planar carpet scraping machine and the spatial RSSR (where R and S stand for revolute and spherical, respectively) mechanism. [DOI: 10.1115/1.2779890]

Keywords: constraint wrench, dynamics, multibody systems, carpet scraping machine, RSSR mechanism

1 Introduction

There are two basic problems associated with the dynamic behavior of multibody systems. The first problem, called forward dynamics, is to determine the motion of a system for a set of applied moments and forces. The second one is the problem of determining the forces required to produce a prescribed motion, as well as the constrained wrenches, i.e., the reaction moments and forces at the joints. Such problem is referred to as inverse dynamics. The forward dynamics is essential to predict the system's behavior. On the other hand, the constraint wrench analysis is valuable for many reasons. It has important applications in control of multibody systems, where the driving torques/forces to follow specified trajectory are evaluated. It also finds applications in designing the supports, joints, and machine components, where information of the bearing reactions is needed to calculate the stresses induced and fatigue characteristics in the machine components.

A great number and variety of formulations of the governing equations of motion for constrained multibody systems have been developed since the period of Lagrange [1–5]. The complexities in formulation of a dynamics problem lie with the proper selection of the coordinates and basic principles of mechanics, i.e., Newton–Euler equations, D'Alembert principle, virtual work, Lagrange equations, energy methods, and others. In the past four decades, researchers focused mainly on the automatic derivation of the equations of motion and their solution strategies [6–20]. Broadly, these formalisms can be classified into three categories, namely, the Newton–Euler (NE) approach [4–8], the Euler–Lagrange (EL) approach [9], and the Kane method [9,10].

The governing equations of motion of a multibody system are differential algebraic equations (DAEs) or ordinary differential equations (ODEs) depending on the coordinates chosen and the basic principles of mechanics used. The DAE formulation is straightforward, as it uses the absolute Cartesian coordinates to define the system's configuration with respect to an inertial reference frame. However, a large number of nonlinear algebraic kinematic constraint equations have to be handled with the differential equations of motion. The solution of DAE provides direct information of the reaction moments/forces at all the joints. However, irrespective of the substantial progress in solving DAEs, they are still regarded as computationally inefficient, inaccurate, and unstable [3,4]. This is due to the large dimension of the DAEs and the associated constraint violation problem [11,12]. Another approach is to use the ODE formulations for dynamic analysis. The ODE formulation relies on independent generalized coordinates, which requires numerical methods to separate independent coordinates from dependent ones.

Several semirecursive formulations for closed-loop systems have been developed [6–8,13–17,21,22] along with the DAE and ODE approaches. Such formulations are based on the velocity transformation methods where the simplicity of the formulation in Cartesian coordinates and the efficiency of the formulation in joint coordinates are maintained. In velocity transformation methods, the equations of motion are first derived in terms of the Cartesian coordinates, which are then transformed into a set of equations of motion in terms of the relative joint coordinates using a velocity transformation matrix [8,13], spatial operators [14,15], or an orthogonal complement [7,20]. For open-loop systems, the relative joint coordinates are independent. Consequently, the conversion of large number of unconstrained equations of motion to a reduced form of constrained equations is straightforward. For the closed-loop systems, however, the relative joint coordinates are not independent because they have to satisfy the loop-closure constraints. Usually, the cut-joint methodology is used to open the closed kinematic loops by incorporating the unknown Lagrange multipliers at the cut joints. One such methodology is proposed in this paper, for constraint wrench evaluation of closed-loop multibody systems.

Copyright © 2007 by ASME
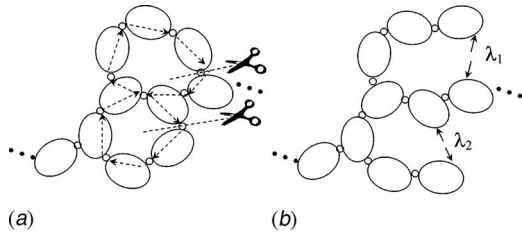
Fig. 1 Closed loops of a multiloop system: (a) the closed loops and (b) its open loops

Fig. 2 A spanning tree

For the evaluation of constraint wrenches, one writes the unconstrained NE equations of motion for all the uncoupled bodies of the system at hand, be it open or closed, and solve for the unknown reaction moments and forces, and the driving torques/forces simultaneously. For complex systems, this leads to a very large number of equations. Hence, efficient recursive algorithms are proposed in Refs. [14,16,23] for the open-loop systems, which cannot be extended in a straight manner to a closed-loop systems [17,18]. As a result, a concept of subsystem recursion is introduced in this paper, where a spanning tree, resulting from cut of the appropriate joints in a closed-loop system, is decomposed into determinate and indeterminate open-loop subsystems, as explained in Sec. 2. Next, the constrained equations of motion for the determinate subsystems are derived and solved for the Lagrange multipliers representing the constraint wrenches at the cut joints, and the driving torques/forces, if any. Interestingly, the determination of the Lagrange multipliers makes some of the indeterminate subsystems determinate, and the process is repeated. The above two steps are referred here as the subsystem recursion. Finally, the constraint wrenches at the uncut joints are calculated using one of the recursion algorithms for open-loop systems, namely, Ref. [23], which is referred here as the body recursion. The subsystem recursion and body recursion together are the two-level recursions mentioned in the title and other places of this paper.

This paper is organized as follows: Sec. 2 explains the spanning tree and its subsystems. Section 3 derives the unconstrained and constrained equations of motion for the subsystems and the whole system. The decoupled natural orthogonal complement matrices used to obtain constrained equations from unconstrained equations are then derived in Sec. 3 for the tree-type subsystems followed by the constraint wrench algorithm in Sec. 5. Two illustrations using the multiloop carpet scraping machine and the spatial RSSR (where R and S stand for revolute and spherical, respectively) mechanism are given in Sec. 6, followed by the conclusions in Sec. 7.

2 Subsystems and Their Classifications

Assume that there are one or more closed kinematic loops in a closed-loop system under study, as shown in Fig. 1(a). In order to convert such multiloop system into an equivalent open-loop system, the closed kinematic loops are cut at some joints, as indicated in Fig. 1(a). Its open loops are shown in Fig. 1(b).

For a complex multiloop system, the joints to be cut can be identified using the graph theory approach [24,25], whereas dependent cut-joint constraints can be eliminated using the screw system of the kinematic loops [26]. The resulting cut system is called the spanning tree of the original closed-loop system, as illustrated in Fig. 2. The distinct branches of the spanning tree, which originate from the base body, #0, are referred to as "subsystems," which could be either serial or tree type. For the purpose of defining the architecture of the spanning tree, base body is generally chosen as the fixed body of the system under study. Any other body whose position, velocity, and acceleration are known can also be selected as the base body.
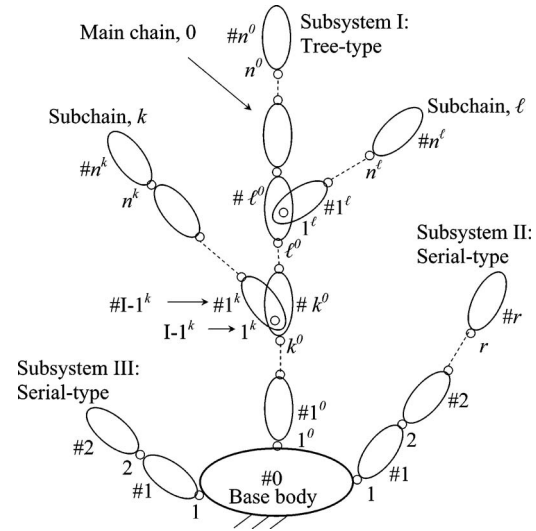
Numbering of the bodies in the spanning tree is based on identifying the serial chain in the system. For serial subsystems, the bodies are numbered from #1 that is connected to the base body, as indicated in Fig. 2. For a tree-type subsystem, the longest chain from the base body, #0, is called the main chain and has n^0 bodies, whereas all other serial branches are called subchains. The subchains are assumed to be connected to the main chain, as shown in Fig. 2 for subchains k and ℓ.

Any subchain is identified by its base body, e.g., in Subsystem I, the subchain k stems from the kth body of the main chain, i.e., #k^0, and has n^k bodies. If more than one subchains emerge from a body of the main chain, each subchain can be identified by double subscripts. For example, $k1$ and $k2$ can emerge from the kth body of the main chain having n^{k1} and n^{k2} bodies. Similarly, the subchain, ℓ, is connected to the ℓth body of the main chain, #ℓ^0, and has n^ℓ bodies, as shown in Fig. 2. In addition, the Roman numerals are prefixed before the number of a body to recognize a subsystem to which the body belongs. For example, as indicated in Fig. 2, #I-1^k denotes the first body of the kth subchain in Subsystem I, whereas I-1^k denotes the first joint of the kth subchain in Subsystem I. Note that the symbol, "#," is used to distinguish labeling of bodies from that of joints. The index of Subchain is dropped in the serial Subsystems, as in Subsystems II and III, because the main chain has no subchains. Assuming that all joints are of one degree of freedom, and the total number of moving bodies is n, then the degree of freedom (DOF) of the spanning tree is given by

$$\text{DOF} = 6 + \sum_{j=\text{I}}^{s} n_j \qquad (1)$$

where n_j is the number bodies in the jth subsystem with the base body having 6DOF. Moreover, s denotes the number of subsystems. For the spanning tree shown in Fig. 2, $n_\text{I}=n^0+n^k+n^\ell$, $n_\text{II}=r$, $n_\text{III}=2$, and hence, $n=n_\text{I}+n_\text{II}+n_\text{III}$.

On a free body in the spanning tree of Fig. 2, there may be as many as four categories of moments and forces or wrenches acting on it, namely, (1) external wrench from the environment that are external to the system, and those provided by the actuators to the system; (2) inertia wrench due to the motion of the body; (3) Lagrange multipliers representing the constraint or reaction wrench at the cut joints; and (4) the constraint or reaction wrench at the uncut joints. For a nonredundant spanning tree resulting from the closed-loop system, the total number of unknowns, namely, the Lagrange multipliers and the driving torques/forces, is equal to the DOF of the spanning tree. Such a spanning tree is
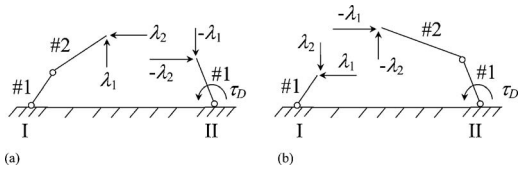
Fig. 3 Open systems for four-bar mechanism

referred here as a determinate system. For example, any spanning tree of the four-bar mechanism, as shown in Fig. 3, is determinate, as it has three unknowns, namely, λ_1, λ_2, and τ_D, and 3DOF. Following the above definition, any subsystem originating from the base body of the spanning tree can also be categorized as *determinate*. The determinate subsystem is the one in which the number of unknowns, i.e., the Lagrange multipliers and the driving torques/forces associated with the subsystem, is equal to its DOF. If the condition for the determinate is not satisfied, then the subsystem is called *indeterminate*. It can be shown that once the unknowns for the determinate subsystems are solved, one or more of the remaining indeterminate subsystem(s) converted into determinate one. For example, there are two spanning trees shown in Fig. 3 for the four-bar mechanism depending on which joint cut. In Fig. 3(*a*), Subsystems I and II are determinate and indeterminate, respectively. Subsystem I has two unknowns, λ_1 and λ_2, with 2DOF whereas Subsystem II has three unknowns, λ_1, λ_2, and τ_D, with 1DOF. Alternatively, in Fig. 3(*b*), both subsystems are indeterminate.

3 Equations of Motion

In this section, a methodology for the constraint wrench formulation of a closed-loop system is presented. First, the closed-loop system is converted into a spanning tree by cutting the appropriate joints of the closed loops, presented in Sec. 2. The loop-closure constraints are then incorporated into the equations of motion as Lagrange multipliers. The equations of motion for the subsystems and the spanning tree are then systematically derived, as explained next.

3.1 Subsystem. The NE equations of motion for the *i*th rigid body, Fig. 4, of *j*th subsystem are given with respect to its origin, O_i, in the fixed inertial frame, as [27]

$$\mathbf{M}_i \dot{\mathbf{t}}_i + \mathbf{W}_i \mathbf{M}_i \mathbf{E}_i \mathbf{t}_i = \mathbf{w}_i \tag{2}$$

where the 6×6 matrices of the mass, $\mathbf{M}_i$, the angular velocity, $\mathbf{W}_i$, and the coupling term, $\mathbf{E}_i$, are as follows:
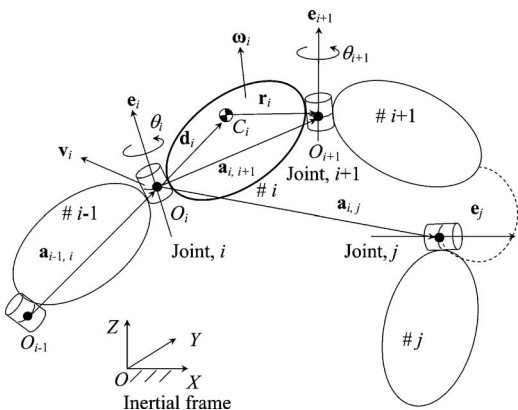

Fig. 4 Coupled bodies

$$\mathbf{M}_i \equiv \begin{bmatrix} \mathbf{I}_i & m_i \tilde{\mathbf{d}}_i \\ -m_i \tilde{\mathbf{d}}_i & m_i \mathbf{1} \end{bmatrix} \quad \mathbf{W}_i \equiv \begin{bmatrix} \tilde{\boldsymbol{\omega}}_i & \mathbf{O} \\ \mathbf{O} & \tilde{\boldsymbol{\omega}}_i \end{bmatrix} \quad \text{and} \quad \mathbf{E}_i \equiv \begin{bmatrix} \mathbf{1} & \mathbf{O} \\ \mathbf{O} & \mathbf{O} \end{bmatrix} \tag{3}$$

in which the 3×3 skew-symmetric matrix, $\tilde{\mathbf{d}}_i$ and $\tilde{\boldsymbol{\omega}}_i$, are associated with the three vectors, $\mathbf{d}_i$ and $\boldsymbol{\omega}_i$, respectively, i.e., $\tilde{\mathbf{d}}_i \mathbf{x} = \mathbf{d}_i \times \mathbf{x}$, and $\tilde{\boldsymbol{\omega}}_i \mathbf{x} = \boldsymbol{\omega}_i \times \mathbf{x}$ for the 3-vector,[1] $\mathbf{x}$. Moreover, $\mathbf{I}_i$ is the 3×3 inertia tensor with respect to the origin, O_i, and $\mathbf{1}$ and $\mathbf{O}$ are the 3×3 identity and zero matrices, respectively. Note that O_i and O_{i+1} are the points where the *i*th body is coupled with its previous, $(i-1)$st, and succeeding, $(i+1)$st, bodies. Furthermore, the 6-vector of twist, $\mathbf{t}_i$, and wrench, $\mathbf{w}_i$, are defined as

$$\mathbf{t}_i \equiv \begin{bmatrix} \boldsymbol{\omega}_i \\ \mathbf{v}_i \end{bmatrix} \quad \mathbf{w}_i \equiv \begin{bmatrix} \mathbf{n}_i \\ \mathbf{f}_i \end{bmatrix} \tag{4}$$

in which $\boldsymbol{\omega}_i$, $\mathbf{v}_i$, $\mathbf{n}_i$, and $\mathbf{f}_i$ are the angular velocity, linear velocity, resultant of external moments, and the resultant of external forces, respectively, at O_i of the *i*th body. For the subsystem *j* having n_j moving bodies, the $6n_j$ scalar unconstrained equations of motion are now expressed as

$$\mathbf{M}_j \dot{\mathbf{t}}_j + \mathbf{W}_j \mathbf{M}_j \mathbf{E}_j \mathbf{t}_j = \mathbf{w}_j \tag{5}$$

where the $6n_j$-vectors $\mathbf{t}_j$, $\dot{\mathbf{t}}_j$, and $\mathbf{w}_j$, respectively, are the generalized twist, twist rate, and wrench, whereas the $6n_j \times 6n_j$ matrices, $\mathbf{M}_j$, $\mathbf{W}_j$, and $\mathbf{E}_j$, are the generalized mass, angular velocity, and coupling matrices, respectively. For a serial subsystem, the bodies are numbered from 1 to n_j, hence, the $6n_j$ vectors, $\mathbf{t}_j$, $\dot{\mathbf{t}}_j$, and $\mathbf{w}_j$, and the $6n_j \times 6n_j$ matrices, $\mathbf{M}_j$, $\mathbf{W}_j$, and $\mathbf{E}_j$, are defined as

$$\mathbf{t}_j \equiv \begin{bmatrix} \mathbf{t}_1 \\ \vdots \\ \mathbf{t}_{n_j} \end{bmatrix} \quad \dot{\mathbf{t}}_j \equiv \begin{bmatrix} \dot{\mathbf{t}}_1 \\ \vdots \\ \dot{\mathbf{t}}_{n_j} \end{bmatrix} \quad \mathbf{w}_j \equiv \begin{bmatrix} \mathbf{w}_1 \\ \vdots \\ \mathbf{w}_{n_j} \end{bmatrix}$$

and

$$\mathbf{M}_j \equiv \text{diag}[\mathbf{M}_1 \ \cdots \ \mathbf{M}_{n_j}] \quad \mathbf{W}_j \equiv \text{diag}[\mathbf{W}_1 \ \cdots \ \mathbf{W}_{n_j}]$$
$$\text{and} \quad \mathbf{E}_j \equiv \text{diag}[\mathbf{E}_1 \ \cdots \ \mathbf{E}_{n_j}] \tag{6}$$

For the tree-type subsystem, i.e., Subsystem I of Fig. 2, bodies are numbered from 1 to n_j, as explained in Sec. 2. The $6n_j$-vectors, $\mathbf{t}_j$, $\dot{\mathbf{t}}_j$, and $\mathbf{w}_j$, and the $6n_j \times 6n_j$ matrices, $\mathbf{M}_j$, $\mathbf{W}_j$, and $\mathbf{E}_j$, are defined as

$$\mathbf{t} \equiv \begin{bmatrix} \mathbf{t}^0 \\ \mathbf{t}^k \\ \mathbf{t}^\ell \end{bmatrix} \quad \dot{\mathbf{t}} \equiv \begin{bmatrix} \dot{\mathbf{t}}^0 \\ \dot{\mathbf{t}}^k \\ \dot{\mathbf{t}}^\ell \end{bmatrix} \quad \mathbf{w} \equiv \begin{bmatrix} \mathbf{w}^0 \\ \mathbf{w}^k \\ \mathbf{w}^\ell \end{bmatrix}$$

and

$$\mathbf{M}_j \equiv \text{diag}[\mathbf{M}^0 \ \mathbf{M}^k \ \mathbf{M}^\ell] \quad \mathbf{W}_j \equiv \text{diag}[\mathbf{W}^0 \ \mathbf{W}^k \ \mathbf{W}^\ell]$$
$$\text{and} \quad \mathbf{E}_j \equiv \text{diag}[\mathbf{E}^0 \ \mathbf{E}^k \ \mathbf{E}^\ell] \tag{7}$$

where the components of vectors and matrices are of sizes according to the serial subchains in the tree-type subsystem. For example, $\mathbf{t}^0$ and $\mathbf{M}^0$ are $6n^0$-vector and $6n^0 \times 6n^0$ matrix, respectively. Note that in Eq. (2) or (5) the wrench, $\mathbf{w}_i$, for the *i*th body is composed of the wrenches, $\mathbf{w}_i^e$, due to externally applied moments and forces on it including those provided by the driving actuators, $\mathbf{w}_i^c$, due to the nonworking constraint moments and forces at the uncut joints, and $\mathbf{w}_i^\lambda$, representing the constraint moments and forces at the cut joints, i.e., $\mathbf{w}_i \equiv \mathbf{w}_i^e + \mathbf{w}_i^c + \mathbf{w}_i^\lambda$. Equation (5) is now rewritten as

---

[1]Note that *n*-vector represents *n* dimensional vector.

$$\mathbf{M}_j \dot{\mathbf{t}}_j + \mathbf{M}_j \mathbf{W}_j \mathbf{t}_j = \mathbf{w}_j^e + \mathbf{w}_j^c + \mathbf{w}_j^\lambda \qquad (8)$$

where $\mathbf{w}_j^e$, $\mathbf{w}_j^c$, and $\mathbf{w}_j^\lambda$ denote the $6n_j$-vectors of corresponding wrenches associated with the jth subsystem. It can be shown that the premultiplication of the transpose of the natural orthogonal complement (NOC) matrix, $\mathbf{N}_j$, associated with velocity constraint of the subsystem [28,29], with the unconstrained NE equations of motion, Eq. (8), leads to a set of n_j constrained equations of motion free from the constraint wrenches at the uncut joints, i.e.,

$$\mathbf{N}_j^T (\mathbf{M}_j \dot{\mathbf{t}}_j + \mathbf{W}_j \mathbf{M}_j \mathbf{E}_j \mathbf{t}_j) = \mathbf{N}_j^T (\mathbf{w}_j^e + \mathbf{w}_j^\lambda) \qquad (9)$$

where the term, $\mathbf{N}_j^T \mathbf{w}_j^c$, vanishes. Note that the size of the NOC matrix, $\mathbf{N}_j$, as derived in Sec. 4, is $6n_j \times n_j$ if all n_j moving bodies of the jth subsystem are coupled with 1DOF joints. Now, introducing the notation for the inertia wrench of the jth subsystem as $\mathbf{w}_j^*$, i.e., $\mathbf{M}_j \dot{\mathbf{t}}_j + \mathbf{W}_j \mathbf{M}_j \mathbf{E}_j \mathbf{t}_j \equiv \mathbf{w}_j^*$, Eq. (9) is rewritten as

$$\mathbf{N}_j^T \mathbf{w}_j^* = \boldsymbol{\tau}_j^e + \boldsymbol{\tau}_j^\lambda \qquad (10)$$

where $\boldsymbol{\tau}_j^e \equiv \mathbf{N}_j^T \mathbf{w}_j^e$ is the n_j-vector of generalized forces due to the external moments and forces, and those resulting from the actuators, gravity, and dissipation, and $\boldsymbol{\tau}_j^\lambda \equiv \mathbf{N}_j^T \mathbf{w}_j^\lambda$ is the n_j-vector of generalized forces due to the constraint moments and forces at the cut joints, i.e., the Lagrange multipliers.

Equation (10) is what many authors obtained using Euler–Lagrange's equations of motion [28]. The n_j scalar equations, Eq. (10), are the linear algebraic equations in Lagrange multipliers and the driving torques/forces associated with the jth subsystem. The number of constrained dynamic equations of motion, n_j, is certainly smaller than the $6n_j$ unconstrained NE equations of motion, Eq. (5). For determinate subsystem, n_j is equal to the number of unknown Lagrange multipliers and the driving torques/forces, if any, that are associated with it and can be solved uniquely. With the unknowns solved for the determinate subsystems, some or all the indeterminate subsystems become determinate, and the process can be repeated. This is referred in this paper as subsystem level recursion. Next, to also obtain the constraint wrenches at the uncut joints, the recursive algorithm for the open-loop system, as proposed in Ref. [23], can be used, i.e.,

$$\mathbf{w}_{i-1,i} = \mathbf{A}_{i,i+1}' \mathbf{w}_{i,i+1} + \mathbf{w}_i^* - \mathbf{w}_i^e \qquad (11)$$

where

$$\mathbf{w}_{i-1,i} \equiv \begin{bmatrix} \mathbf{n}_{i-1,i} \\ \mathbf{f}_{i-1,i} \end{bmatrix} \quad \mathbf{w}_i^* \equiv \begin{bmatrix} \mathbf{n}_i^* \\ \mathbf{f}_i^* \end{bmatrix}$$

The moment, $\mathbf{n}_{i-1,i}$, and the force, $\mathbf{f}_{i-1,i}$, are those applied by the $(i-1)$st body to the ith one at the ith joint and so on. In Eq. (11), the 6×6 matrix, $\mathbf{A}_{i,i+1}'$, is the *wrench propagation matrix*, which transforms the wrench acting at point O_{i+1} to O_i of the ith body, i.e.,

$$\mathbf{A}_{i,i+1}' \equiv \begin{bmatrix} \mathbf{1} & \tilde{\mathbf{a}}_{i,i+1} \\ \mathbf{O} & \mathbf{1} \end{bmatrix} \qquad (12)$$

where $\tilde{\mathbf{a}}_{i,i+1}$ is the 3×3 skew-symmetric matrix associated with the 3-vector, $\mathbf{a}_{i,i+1}$, as shown in Fig. 4. Equation (11) is referred here as the body-level recursion. The above two recursions together are called the two-level recursions. This approach is, however, termed as the subsystem approach, where Eqs. (10) and (11) are used.

3.2 Spanning Tree. For the spanning tree, the constrained equations are obtained using Eq. (10) as

$$\mathbf{N}_j^T \mathbf{w}_j^* = \boldsymbol{\tau}_j^e + \boldsymbol{\tau}_j^\lambda \quad \text{for } j = \text{I}, \dots, s \qquad (13)$$

where s is the number of subsystems, which can be either serial or tree type originating from the base body of the spanning tree. Equation (13) is written in a compact form as

$$\mathbf{N}^T \mathbf{w}^* = \boldsymbol{\tau}^e + \boldsymbol{\tau}^\lambda \qquad (14)$$

where

$$\mathbf{w}^* \equiv \begin{bmatrix} \mathbf{w}_I^* \\ \vdots \\ \mathbf{w}_s^* \end{bmatrix} \quad \boldsymbol{\tau}^e \equiv \begin{bmatrix} \boldsymbol{\tau}_I^e \\ \vdots \\ \boldsymbol{\tau}_s^e \end{bmatrix} \quad \text{and} \quad \boldsymbol{\tau}^\lambda \equiv \begin{bmatrix} \boldsymbol{\tau}_I^\lambda \\ \vdots \\ \boldsymbol{\tau}_s^\lambda \end{bmatrix} \qquad (15)$$

and $\mathbf{N}$ is the $6n \times n$ NOC matrix for the spanning tree, which is

$$\mathbf{N} = \text{diag}(\mathbf{N}_I \cdots \mathbf{N}_s) \qquad (16)$$

in which $\mathbf{N}_j$ is the NOC matrix for the jth subsystem be it a serial or tree type, derived next in Sec. 4. Moreover, $\mathbf{w}^*$ is the $6n$-vector, and $\boldsymbol{\tau}^e$ and $\boldsymbol{\tau}^\lambda$ are the n-vectors—$n \equiv n_I + \cdots + n_S$ being the total number bodies in the spanning tree. For a nonredundant spanning tree resulting from the closed-loop system, the total number of unknowns, the driving torques/forces, and the Lagrange multipliers is equal to the total number of bodies, n, and the DOF of the system. Hence, the scalar equations of Eq. (14) can be solved using any standard method such as lower/upper triangular (LU) decomposition [30], whereas the constraint wrenches at the uncut joints are solved using the body-level recursions, namely, Eq. (11). This approach is termed here as the system approach, where Eqs. (10) and (14) are used. Similar methodology is also reported in Refs. [7,15,17,31].

4 Natural Orthogonal Complement Matrix

The NOC matrix [28] is used to derive the constrained equations of motion, Eqs. (10) and (14), for a subsystem and the spanning tree, respectively. For the serial-type subsystem, the NOC matrix can be obtained as the multiplication of two block matrices, called the decoupled natural orthogonal complement (De-NOC) matrices [20], whereas for tree-type subsystem, it is derived in this paper. Note here that the DeNOC matrices for closed-loop parallel-type system in Refs. [27,32] cannot be used here, as they were derived considering the special architecture without cutting them.

Referring to Fig. 4, the twist, $\mathbf{t}_i$, as defined in Eq. (4), is expressed in terms of the twist of its previous body, i.e., the $(i-1)$st one, $\mathbf{t}_{i-1}$, as [19]

$$\mathbf{t}_i = \mathbf{A}_{i,i-1} \mathbf{t}_{i-1} + \mathbf{p}_i \dot{\theta}_i \qquad (17)$$

where the 6×6 matrix, $\mathbf{A}_{i,i-1}$, is called the *twist propagation matrix*, which transforms the twist of the $(i-1)$st body to the ith one as if they are rigidly connected. The matrix, $\mathbf{A}_{i,i-1}$, is given by

$$\mathbf{A}_{i,i-1} \equiv \begin{bmatrix} \mathbf{1} & \mathbf{O} \\ \tilde{\mathbf{a}}_{i,i-1} & \mathbf{1} \end{bmatrix} \qquad (18)$$

in which the 3×3 skew-symmetric matrix, $\tilde{\mathbf{a}}_{i,i-1}$, is associated with the 3-vector $\mathbf{a}_{i,i-1}$. For serially connected three bodies, namely, i, j, and k, the twist propagation matrices satisfy the following properties:

$$\mathbf{A}_{ij} \mathbf{A}_{jk} = \mathbf{A}_{ik} \quad \mathbf{A}_{ii} = \mathbf{1} \quad \mathbf{A}_{ij}^{-1} = \mathbf{A}_{ji} \quad \text{and} \quad \det(\mathbf{A}_{ij}) = 1 \qquad (19)$$

The scalar, $\dot{\theta}_i$ of Eq. (17), is the joint rate. For a revolute joint, θ_i is the variable parameter and the angle of the ith body moved with respect to the $(i-1)$st one. For a prismatic joint, $\dot{\theta}_i$ is the linear speed of the point O_i with respect to O_{i-1}. In Eq. (17), the six vectors, $\mathbf{p}_i$, take into account the motion of the ith body relative to the $(i-1)$st one, which is dependent on the DOF of the ith joint, and is called the *joint-rate propagation vector*. For 1DOF joints, e.g., a revolute or a prismatic,

$$\mathbf{p}_i \equiv \begin{bmatrix} \mathbf{e}_i \\ \mathbf{0} \end{bmatrix} \text{ revolute joint } \quad \text{and} \quad \mathbf{p}_i \equiv \begin{bmatrix} \mathbf{0} \\ \mathbf{e}_i \end{bmatrix} \text{ prismatic joint}$$

$$(20)$$

Other joints, e.g., spherical, screw, etc., can be treated as the combination of revolute and prismatic joints [27]. In Eq. (20), the

3-vector, $\mathbf{e}_i$, represent the unit vector along the axis of the rotation of the revolute joint or along the direction of the linear motion of the prismatic joint, respectively. Also, the matrix $\mathbf{O}$ and the vector $\mathbf{0}$ in Eqs. (18) and (20), respectively, are the 3×3 matrix and 3-vector of zeros, and the matrix $\mathbf{1}$ is the 3×3 identity matrix. Henceforth, they will be understood to be compatible sizes based on where they appear.

For the serial system having n moving bodies, writing Eq. (17), for $i=1, \ldots, n$, and expressing them in a compact form yield

$$\mathbf{A}_0 \mathbf{t}_0 + \mathbf{A} \mathbf{t} = \mathbf{N}_d \dot{\boldsymbol{\theta}} \qquad (21)$$

where the $6n \times 6$, $6n \times 6n$, and $6n \times n$ matrices, $\mathbf{A}_0$, $\mathbf{A}$, and $\mathbf{N}_d$, are defined as

$$\mathbf{A}_0 \equiv \begin{bmatrix} -\mathbf{A}_{10} \\ \mathbf{O} \\ \vdots \\ \mathbf{O} \end{bmatrix} \quad \mathbf{A} \equiv \begin{bmatrix} \mathbf{1} & \mathbf{O} & \cdots & \mathbf{O} & \mathbf{O} \\ -\mathbf{A}_{21} & \mathbf{1} & \cdots & \mathbf{O} & \mathbf{O} \\ \vdots & \vdots & \ddots & \vdots & \vdots \\ \mathbf{O} & \mathbf{O} & \cdots & -\mathbf{A}_{n,n-1} & \mathbf{1} \end{bmatrix}$$

$$\text{and} \quad \mathbf{N}_d \equiv \text{diag}\begin{bmatrix} \mathbf{p}_1 & \cdots & \mathbf{p}_n \end{bmatrix} \qquad (22)$$

Also, the $6n$-vector of generalized twist, $\mathbf{t}$, and the n-vector of generalized joint rate, $\dot{\boldsymbol{\theta}}$, are defined as

$$\mathbf{t} \equiv [\mathbf{t}_1^T \cdots \mathbf{t}_n^T]^T \quad \text{and} \quad \dot{\boldsymbol{\theta}} \equiv [\dot{\theta}_1 \cdots \dot{\theta}_n]^T \qquad (23)$$

The generalized twist, $\mathbf{t}$, is then obtained from Eq. (21) by inverting the matrix, $\mathbf{A}$, as

$$\mathbf{t} = -\mathbf{N}_l \mathbf{A}_0 \mathbf{t}_0 + \mathbf{N}_l \mathbf{N}_d \dot{\boldsymbol{\theta}} \qquad (24)$$

where

$$\mathbf{N}_l \equiv \mathbf{A}^{-1} = \begin{bmatrix} \mathbf{1} & \mathbf{O} & \cdots & \mathbf{O} \\ \mathbf{A}_{21} & \mathbf{1} & \vdots & \mathbf{O} \\ \vdots & \vdots & \ddots & \vdots \\ \mathbf{A}_{n1} & \mathbf{A}_{n2} & \cdots & \mathbf{1} \end{bmatrix} \qquad (25)$$

where $\mathbf{A}_{i,j} = \mathbf{A}_{i,i-1} \cdots \mathbf{A}_{j+1,j}$ for $i > j$. For the serial-type system, if the base body is fixed, i.e., $\mathbf{t}_0 = \mathbf{0}$, Eq. (24) takes the following simple form:

$$\mathbf{t} = \mathbf{N} \dot{\boldsymbol{\theta}} \quad \text{where} \quad \mathbf{N} \equiv \mathbf{N}_l \mathbf{N}_d \qquad (26)$$

in which the $6n \times 6n$ lower block triangular matrix, $\mathbf{N}_l$, and the $6n \times n$ block diagonal matrix, $\mathbf{N}_d$, are called the DeNOC matrices [19], whereas $\mathbf{N}$ is the NOC matrix [28]. The DeNOC matrices, $\mathbf{N}_l$ and $\mathbf{N}_d$, are nothing but the spatial operators of Rodriguez et al. [15]. They separate the architecture information of the bodies from that of the joints. For example, if the ith joint is locked, $\dot{\theta}_i$ is zero, and the matrix, $\mathbf{A}_{i,i-1}$, transfers the twist of #$(i-1)$ to #i, as if they have formed a rigid composite body.

Referring to the tree-type system of Fig. 2, i.e., Subsystem I, the generalized twist, for the main chain, denoted as $\mathbf{t}^0$, is obtained from Eq. (26) as

$$\mathbf{t}^0 = \mathbf{N}_l^0 \mathbf{N}_d^0 \dot{\boldsymbol{\theta}}^0 \qquad (27)$$

where superscript "0" indicates the main chain mentioned in Sec. 2. Using Eq. (24), the $6n^k$ vector of the generalized twist for the kth subchain of Subsystem I, $\mathbf{t}^k$, is given by

$$\mathbf{t}^k = -\mathbf{N}_l^k \mathbf{A}_0^k \mathbf{t}_0^k + \mathbf{N}_l^k \mathbf{N}_d^k \dot{\boldsymbol{\theta}}^k \qquad (28)$$

where the $6n^k \times 6n^k$ matrix, $\mathbf{N}_l^k$, and the $6n^k \times n^k$ matrix $\mathbf{N}_d^k$ are the DeNOC matrices of the kth subchain, and $\mathbf{t}_0^k \equiv \mathbf{t}_k^0$ is nothing but the twist of the kth body in the main chain, 0. The twist, $\mathbf{t}_k^0$, can be obtained from Eq. (27) as

$$\mathbf{t}_k^0 = \mathbf{N}_{lk}^0 \mathbf{N}_d^0 \dot{\boldsymbol{\theta}}^0 \qquad (29)$$

where the $6 \times 6n^0$ matrix, $\mathbf{N}_{lk}^0$, is given by

$$\mathbf{N}_{lk}^0 \equiv [\mathbf{A}_{k,1}^0 \cdots \mathbf{A}_{k,k-1}^0 \ \mathbf{1} \ \mathbf{O} \cdots \mathbf{O}] \qquad (30)$$

Substituting Eq. (29) into Eq. (28) yields

$$\mathbf{t}^k = \mathbf{N}_l^{k0} \mathbf{N}_d^0 \dot{\boldsymbol{\theta}}^0 + \mathbf{N}_l^k \mathbf{N}_d^k \dot{\boldsymbol{\theta}}^k \quad \text{where} \quad \mathbf{N}_l^{k0} \equiv -\mathbf{N}_l^k \mathbf{A}_0^k \mathbf{N}_{lk}^0 \qquad (31)$$

For other subchains, one can similarly obtain Eq. (31). Now, generalized twist for the tree-type Subsystem I, Fig. 2, i.e., the $6n$ vector, $\mathbf{t}$, can be expressed as

$$\mathbf{t} = \mathbf{N} \dot{\boldsymbol{\theta}} \quad \text{where} \quad \mathbf{N} \equiv \mathbf{N}_l \mathbf{N}_d \qquad (32)$$

where $n \equiv n^0 + n^k + n^\ell$ being the total number of moving bodies in the tree-type system and the $6n$-vector, $\mathbf{t}$, n-vector, $\dot{\boldsymbol{\theta}}$, the $6n \times 6n$ matrix, $\mathbf{N}_l$, and the $6n \times n$ matrix, $\mathbf{N}_d$, are defined by

$$\mathbf{t} \equiv \begin{bmatrix} \mathbf{t}^0 \\ \mathbf{t}^k \\ \mathbf{t}^\ell \end{bmatrix} \quad \dot{\boldsymbol{\theta}} \equiv \begin{bmatrix} \dot{\boldsymbol{\theta}}^0 \\ \dot{\boldsymbol{\theta}}^k \\ \dot{\boldsymbol{\theta}}^\ell \end{bmatrix} \quad \mathbf{N}_l \equiv \begin{bmatrix} \mathbf{N}_l^0 & \mathbf{O} & \mathbf{O} \\ \mathbf{N}_l^{k0} & \mathbf{N}_l^k & \mathbf{O} \\ \mathbf{N}_l^{\ell 0} & \mathbf{O} & \mathbf{N}_l^\ell \end{bmatrix}$$

$$\text{and} \quad \mathbf{N}_d \equiv \text{diag}[\mathbf{N}_d^0 \ \mathbf{N}_d^k \ \mathbf{N}_d^\ell] \qquad (33)$$

For additional subchains, one can modify the expressions of $\mathbf{t}$, $\dot{\boldsymbol{\theta}}$, $\mathbf{N}_l$, and $\mathbf{N}_d$, as given in Eq. (33). Equations (32) and (33) together provide the DeNOC matrices for the tree-type system at hand, which are used to reduce the dimension of the system's NE equations of motion, as mentioned in Sec. 3.1.

5 Algorithm for Constraint Wrenches

Based on the dynamic analyses presented in Secs. 3 and 4, the methods to compute the constraint wrenches are categorized into the following three categories.

(1) *Traditional method*. In this method, the constraint wrenches and the driving torques/forces at all the joints are solved simultaneously using the $6n$ unconstrained NE equations of motion, Eq. (8). For example, nine equations for the planar four-bar mechanism shown in Fig. 3 are solved using this method.

(2) *System approach*. In this method, all the Lagrange multipliers and the driving torques/forces of a spanning tree of the closed-loop system are solved simultaneously, followed by the body-level recursive calculation of the constraint wrench at the uncut joints. One can find similar approach in Nikravesh and Gim [7], Kim and Vanderploeg [8], Rodriguez et al. [15], Anderson and Critchley [17], Shabana [31], and others. For a four-bar mechanism of Fig. 3(*a*) or 3(*b*), the three constrained equations for each spanning tree are solved simultaneously, followed by recursive calculation of the constraint wrenches at the three uncut joints.

(3) *Subsystem approach*. This method is proposed in this paper. It is a two-level recursive method to compute all the Lagrange multipliers, driving torques/forces, and the constraints wrenches at the uncut joints, as shown in Fig. 5. In the first or subsystem level recursion, the determinate subsystems, as defined in Sec. 2, are identified. The sets of the Lagrange multipliers, and the driving torques/forces, if any, of the determinate systems are solved independently. With the known Lagrange multipliers of the determinate subsystems, some or all of the remaining indeterminate subsystems become determinate for which the above step is repeated. With all the Lagrange multipliers, and the driving torques/forces of the spanning tree known, the constraint wrenches at the uncut joints of the subsystems are determined using body-level recursion. For the four-bar mechanism, Fig. 3(*a*), two constrained equations for Subsystem I are first solved simultaneously, followed by one constrained equation for Subsystem II. Finally, the constraint wrenches at the uncut joints are solved using body-level recursion. The method will not succeed if all the subsystems are indeterminate. Under such circumstances, the system ap-
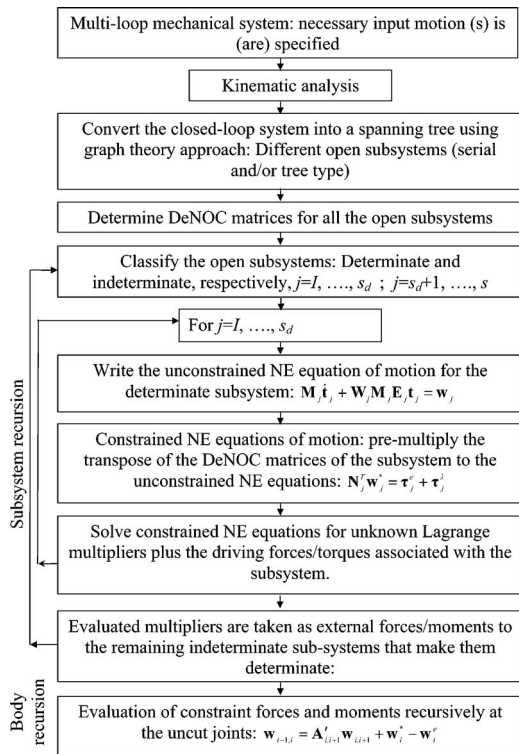
Fig. 5 Constraint wrenches calculation using two-level recursive subsystem approach

proach is used to produce solution. For the four-bar mechanism, Fig. 3(b), three constrained equations are solved simultaneously, as explained in the system approach above.

Advantages of the proposed subsystem approach are highlighted as follows.

(1) For a large number of bodies with many kinematic loops, and repeated calculations, the algorithm has proven to be efficient for the computation of constraint wrenches at all joints. For repetitive calculations, the authors used the proposed subsystem approach in the balancing of shaking force and shaking moment where the dynamic algorithm is repeated several times in an optimization code [33]. The computational aspects are reported in Tables 2 and 3.

(2) It can be used without any modification for the determination of the driving torques/forces only of a closed-loop system necessary for control purposes. Here, the last step of finding the constraint wrenches at the uncut joints need not be carried out.

(3) Since the constraint forces and moments information is available at the subsystem level, it may prove useful to analyze them from mechanical design point of view, as the subsystem level results could provide the clue on how it affects the overall system.

6 Illustrations

In this section, two examples are analyzed to show the effectiveness of the proposed wrench formulation.

6.1 Carpet Scraping Machine. In the first illustration, the carpet scraping machine [34], developed to clean a carpet after it is woven, is taken up. Two mechanisms, namely, the Hoekens four-bar and the Pantograph, are used in the machine, as shown in Fig. 6. The Hoekens mechanism is a crank-rocker mechanism whose coupler generates a partially straight path. The straight line stroke generated by the Hoekens mechanism is magnified by the
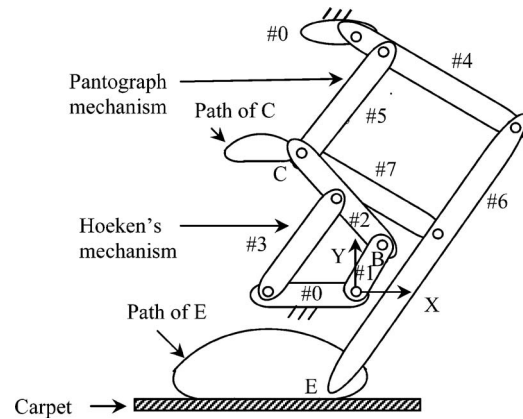

Fig. 6 Carpet scraping mechanism

Pantograph mechanism.

The spanning tree of the mechanism is obtained by cutting the joints between Links #1-#2, #2-#5, and #2-#7, of the closed loops, #0-#1-#2-#3, #0-#1-#2-#5-#4, and #0-#1-#2-#7-#6-#4, respectively. The resulting spanning tree, Fig. 7, has three subsystems, I, II, and III. The links and joints of the subsystems are now numbered as per the scheme described in Sec. 2. For example, Link #3 in Fig. 6 is indicated in Fig. 8 as #1 of Subsystem I, i.e., Link #I-1. Subsystem I has two moving links, #I-1 and #I-2, with 2DOF. Subsystem II has only one moving link, #II-1, which is connected to its previous body, i.e., #0, at joint, II-1. Both the subsystems, I and II, are serial types, whereas Subsystem III is tree type with four moving links numbered as #III-1^0, #III-2^0, #III-3^0, and #III-1^1, which are coupled by four revolute joints denoted as III-1^0, III-2^0, III-3^0, and III-1^1. Note that each subsystem originates from the base body, #0, which is fixed. Moreover, to avoid clumsiness in Fig. 7, the subsystem notations, I, II, and III, are not used in the link and joint numbers. Furthermore, the joint angles θ_1 and θ_2 of Subsystem II, θ_1 of Subsystem I, and $\theta_1^0, \theta_2^1, \theta_3^0, \theta_1^1$ of
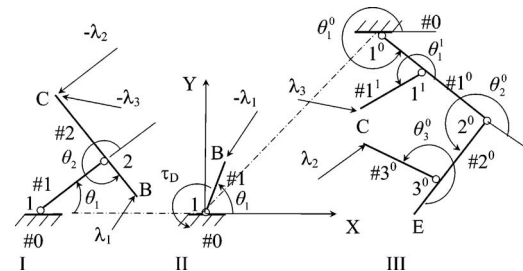

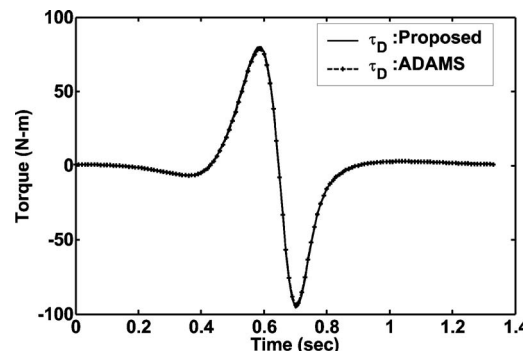Fig. 7 Subsystems of spanning tree for the carpet scraping mechanism

Fig. 8 Comparison of driving torque

Table 1 Link parameters of the scraping machine

Subsystem	Link	Length (m)	Mass (kg)	Moment of inertia at link origin (kg m²) ×10⁻³
I	1	$a_{1,2}=0.115$	3.0	13.30
	2	$a_{2,B}=0.115$	5.0	22.12
II	1	$a_{1,B}=0.038$	1.5	0.73
III	1^0	$a_{12}^0=0.335$	4.2	157.00
	2^{0a}	$a_{23}^0=0.239$	10.5	2449.00
	3^0	$a_{3,c}^0=0.239$	3.0	57.00
	1^1	$a_{1,B}^1=0.239$	3.0	57.00

[a]Extension of link #III-2^0 beyond joint III-2^0 is 0.597 m.

Table 2 Comparison of CPU time in Pentium IV (2.60 GHz). Matrix sizes: traditional, 21×21; system approach, 7×7; subsystem approach, 4×4, 3×3, 1×1.

Methods	Theoretical order of computations	CPU time (s) Dynamic algorithm[a]	CPU time (s) Optimization algorithm[b]
Traditional	$O(21^3/3)=O(3087)$	0.219	118.610
System approach	$O(7^3/3)+O(7\times2)$ $=O(128.3)$	0.156 (30.59)[c]	56.703 (52.19)
Subsystem approach	$O(4^3/3+3^3/3+1)+O(7\times2)$ $=O(45.3)$	0.156 (30.59)	56.703 (52.19)

[a]For simulation time of 1.34 s (i.e., time period of the crank) with a step size of 0.01 s.
[b]For 33 iterations and 1000 function evaluations.
[c]Percentage savings over the traditional method.

Subsystem III are treated as generalized coordinates.

The input motion is provided to Joint 1 of Subsystem II by applying torque τ_D, which needs to be calculated for the known motion of the mechanism. Additionally, three unknown vectors of Lagrange multipliers, $\boldsymbol{\lambda}_i$ for $i=1,2,3$, as indicated in Fig. 7, are

$$\boldsymbol{\lambda}_1=[\lambda_{1x}\ \lambda_{1y}]^T \quad \boldsymbol{\lambda}_2=[\lambda_{2x}\ \lambda_{2y}]^T \quad \text{and} \quad \boldsymbol{\lambda}_3=[\lambda_{3x}\ \lambda_{3y}]^T$$

Being the motion of the mechanism planar, the two components for each Lagrange multiplier represent the reaction forces at the cut revolute joints. Hence, the total number of scalar unknowns is 7, namely, $\lambda_{1x}, \lambda_{1y}, \lambda_{2x}, \lambda_{2y}, \lambda_{3x}, \lambda_{3y}$, and τ_D. Note that the DOF of the spanning tree (Subsystems I, II, and III, plus the base body) is also 7. It implies that one can obtain seven constrained equations of motion, Eq. (14), which can be simultaneously solved for seven unknowns, as in the system approach of Sec. 5. The dimension of the associated matrix is 7×7. Alternatively, Subsystem III has four unknowns, $\lambda_{2x}, \lambda_{2y}, \lambda_{3x}, \lambda_{3y}$, and 4DOF, which allows one to solve for the four unknowns using the four constrained equations of motion for Subsystem III. The associated matrix size is 4×4. In the next step, evaluated $\lambda_{2x}, \lambda_{2y}, \lambda_{3x}, \lambda_{3y}$ are taken as known external forces to Subsystem I that make it determinate, where $\lambda_{1x}, \lambda_{1y}$ are the unknowns and the DOF is 2. Hence, the two unknowns can be solved using the constrained equations of motion for Subsystem I. Now, only τ_D remains as the unknown in Subsystem II, which can be solved by one constrained equation of motion of the subsystem. The above three steps correspond to the subsystem approach of Sec. 5. In the final step, the constraint wrenches in the uncut joints are computed recursively.

6.1.1 Numerical Example. The multiloop scraping mechanism shown in Fig. 6 has the parameters shown in Table 1. They are used here to find the constraint forces at the joints of the mechanism. The input motion provided to Link #II-1 is a constant speed of 45 rpm (4.712 rad/s). The fixed frame, XYZ, is located at Joint II-1, Fig. 7, where axis Z is perpendicular to the page. Joints I-1 and III-1^0 are located at $(-0.089\ m, 0)$ and $(0.038\ m, 0.410\ m)$ respectively. Joint between #I-1 and #I-2 is located at the middle of Link #I-2. Joint III-1^1 is at 0.096 m on Link #III-1^0 from Joint III-1^0.

The constraint forces are now obtained as follows:

(a) The Lagrange multipliers of Subsystem III, namely, λ_{2x}, λ_{2y}, λ_{3x}, and λ_{3y}, are evaluated first.

(b) Taking λ_{2x}, λ_{2y}, λ_{3x}, and λ_{3y} as external forces, the Lagrange multipliers in Subsystem I, namely, λ_{1x} and λ_{1y}, are evaluated next.

(c) Finally, τ_D is evaluated for Subsystem II, shown in Fig. 8. The results are compared with those obtained from the model developed using the commercial software, MSC.ADAMS 2005 (automated dynamic analysis of mechanical systems) [35]. Only the comparison of the driving torque is shown in Fig. 8. However, all other forces

were also compared, which showed exact match but not reported here due to limited space.

6.1.2 Computation Efficiency. In this subsection, a look into the computational efficiency of the proposed two-level recursive subsystem approach is given. Table 2 shows the comparison of the theoretical order of computations and the time taken by the CPU of a Pentium IV computer for the numerical example taken in Sec. 6.1.1. Three methods are considered, namely, the traditional method using the 21×21 matrix, the system approach using the 7×7 matrix and the body-level recursions, and the two-level recursive subsystem approach using the 4×4, 2×2, and 1×1 matrices and the body-level recursions. The CPU time is estimated for 134 positions of the mechanism during one complete rotation of the link, #II-1. The algorithm is also used for the optimization of the shaking force and shaking moment [33]. For the same iterations, the CPU time taken by the optimization process is shown in the last column of Table 2.

A significant reduction in CPU time is observed in both the system and subsystem approaches over the traditional method. This amounts to almost 30% and 52% savings during the constraint force calculations only, and the optimization process, respectively. Note, however, that there is almost no CPU time difference between the system and subsystem approaches. This is mainly due to the planar nature of the system at hand.

6.2 Spatial RSSR Mechanism. In this section, a spatial RSSR mechanism, where R and S stand for revolute and spherical, respectively, is considered, as shown in Fig. 9. The kinematic equivalent of the RSSR mechanism is a 7R mechanism [36], where a spherical joint is considered equivalent to three revolute joints intersecting at a point. In Fig. 9, however, the second spherical joint between Links #1 and #3 is substituted with Hook's joint, which is equivalent to two revolute joints intersecting at a point. This is due to the removal of the redundant rotation of Link #3 about it own axis. The closed-loop mechanism is now made open by cutting the joint between Links #5 and #6 of the 7R mechanism, as shown in Fig. 10. The resulting two open serial-
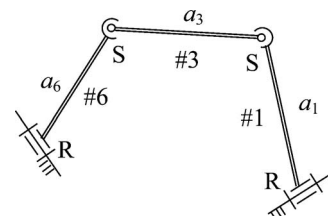

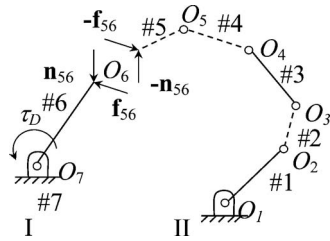**Fig. 9 The RSSR mechanism**

Fig. 10 Spanning tree of the 7R mechanism

type subsystems are Subsystem I with one moving Link #6 and Subsystem II with five serially connected moving links, #1,…,#5, as shown in Fig. 10. Both the subsystems are connected to the fixed link, #0. The four unknowns in the spanning tree of the 7R mechanism are $\mathbf{f}_{56} \equiv [\lambda_x \ \lambda_y \ \lambda_z]^T$ and the driving torque τ_D. Note that $\mathbf{n}_{56} = \mathbf{0}$, as the combination of joints 4, 5, and 6 cannot resist any moment. Also, Links #4 and #5 have zero mass and dimensions. Hence, Subsystem II has effectively three unknowns, λ_x, λ_y, λ_z, and three links, #1, #2, #3, with 3DOF. As a result, three simultaneous constrained equations of motion have to be solved for the unknown Lagrange multipliers. The rest of the analysis is the same as illustrated for the carpet scraping machine, as in Sec. 6.1. The results, i.e., λ_x, λ_y, λ_z, and τ_D, are compared with those available in literature, namely, in Ref. [37], and not reported here due to page restriction.

However, the comparison of the theoretical order of computations and the CPU time taken by a Pentium IV computer is given in Table 3. The proposed two-level recursive subsystem approach performs much better than the other two approaches. The reason is that the time taken for transforming the vectors and matrices for the spatial problem is more for the many bodies, where the recursive methods are known to perform better [38]

7 Conclusions

This paper contributes a new two-level recursive method to find the constraint wrenches, i.e., moments and forces at the joints, of closed-loop systems. In the first level, the subsystems of the spanning tree are considered to solve for their Lagrange multipliers at the cut joints and the driving torques/forces, if any. In the second level, the constraint forces and moments of the bodies in the subsystems are obtained recursively from one body to the next. While the former recursion is referred here as the subsystem recursion, the latter is termed as the body recursion. The complete two-level recursions are called subsystem approach. For the dynamic formulation, the concept of the decoupled orthogonal complement matrices is used here to reduce the dimensions of the unconstrained

Table 3 Comparison of the CPU times in Pentium IV (2.60 GHz). Matrix sizes: traditional, 18×18; system approach, 4×4; subsystem approach, 3×3.

Methods	Theoretical order of computations	CPU time (s)	
		Dynamic algorithm[a]	Optimization algorithm[b]
Traditional	$O(18^3/3) = O(1994)$	0.6560	176.672
System approach	$O(4^3)/3 + O(4 \times 6)$ $= O(45.33)$	0.609 (7.16)[c]	170.125 (3.70)
Subsystem approach	$O(3^3/3) + O(4 \times 6)$ $= O(33)$	0.5960 (9.15)	157.156 (11.04)

[a]For simulation time of 0.6 s (i.e., the time period of the crank) with step size of 0.001 s.
[b]For 21 iterations and 500 function evaluations for each method.
[c]Percentage savings in CPU time.

NE equations of motion. For this purpose, the DeNOC matrices for the tree-type system are derived in this paper for the first time based on the method proposed earlier for the serial- and parallel-type systems. The proposed algorithm is illustrated using two systems, namely, the planar multiloop carpet scraping machine and the spatial RSSR mechanism. The aspect of efficiency is also investigated, which showed that the two-level recursion performs better, particularly, when the closed-loop system is spatial and has many bodies connected through loops, and the computations have to be repeated several times, e.g., in the optimization process.

References

[1] Eberhard, P., and Schiehlen, W., 2006, "Computational Dynamics of Multibody Systems: History, Formalisms, and Applications," ASME J. Comput. Nonlinear Dyn., **1**(1), pp. 3–12.
[2] Roberson, R. E., and Schwertassek, R., 1988, *Dynamics of Multibody Systems*, Springer-Verlag, Berlin.
[3] Schiehlen, W., 1990, *Multibody Systems Handbook*, Springer-Verlag, Berlin.
[4] Shabana, A. A., 2005, *Dynamics of Multibody Systems*, Cambridge University Press, New York.
[5] Paul, B., 1975, "Analytical Dynamics of Mechanisms: A Computer Oriented Overview," Mech. Mach. Theory, **10**, pp. 481–507.
[6] Nikravesh, P. E., 1988, *Computer-Aided Analysis of Mechanical Systems*, Prentice-Hall, Englewood Cliffs, NJ.
[7] Nikravesh, P. E., and Gim, G., 1993, "Systematic Construction of the Equations of Motion for Multibody Systems Containing Closed Kinematic Loops," ASME J. Mech. Des., **115**, pp. 143–149.
[8] Kim, S. S., and Vanderploeg, M. J., 1986, "A General and Efficient Method for Dynamic Analysis of Mechanical Systems Using Velocity Transformation," ASME J. Mech., Transm., Autom. Des., **108**(2), pp. 176–182.
[9] Kane, T. R., and Levinson, D. A., 1983, "Multibody Dynamics," ASME J. Appl. Mech., **50**, pp. 1071–1078.
[10] Huston, R. L., 2005, "Advances in Computational Methods for Multibody System Dynamics," Comput. Model. Eng. Sci., **10**(2), pp. 143–152.
[11] Yen, J., and Petzold, L. R., 1998, "An Efficient Newton-Type Iteration for the Numerical Solution of Highly Oscillatory Constrained Multibody Dynamic Systems," SIAM J. Sci. Comput. (USA), **19**(5), pp. 1513–1534.
[12] Baumgarte, J., 1972, "Stabilization of Constraints and Integrals of Motion," Comput. Methods Appl. Mech. Eng., **1**, pp. 1–16.
[13] Jerkovskey, W., 1978, "The Structure of Multibody Dynamics Equations," J. Guid. Control, **1**(3), pp. 173–182.
[14] Rodriguez, G., Jain, A., and Kreutz-Delgado, K., 1991, "A Spatial Operator Algebra for Manipulator Modeling and Control," Int. J. Robot. Res., **10**(4), pp. 371–381.
[15] Rodriguez, G., Jain, A., and Kreutz-Delgado, K., 1992, "Spatial Operator Algebra for Multibody System Dynamics," J. Astronaut. Sci., **40**(1), pp. 27–50.
[16] Featherstone, R., 1987, *Robot Dynamics Algorithms*, Kluwer Academic, New York.
[17] Anderson, K. S., and Critchley, J. H., 2003, "A Generalized Recursive Coordinate Reduction Method for Multibody System Dynamics," Int. J. Multiscale Comp. Eng., **1**(2&3), pp. 181–199.
[18] Blajer, W., 2004, "On the Determination of Joint Reactions in Multibody Mechanisms," ASME J. Mech. Des., **126**(2), pp. 341–350.
[19] Saha, S. K., 1997, "A Decomposition of the Manipulator Inertia Matrix," IEEE Trans. Rob. Autom., **13**(2), pp. 301–304.
[20] Saha, S. K., 1999, "Dynamics of Serial Multibody Systems Using the Decoupled Natural Orthogonal Complement Matrices," ASME J. Appl. Mech., **66**, pp. 986–996.
[21] Serban, R., and Haug, E. J., 2000, "Globally Independent Coordinates for Real-Time Vehicle Simulation," ASME J. Mech. Des., **122**, pp. 575–582.
[22] Cuadrado, J., Dopico, D., Gonzalez, M., and Naya, M. A., 2004, "A Combined Penalty and Recursive Real-Time Formulation for Multibody Dynamics," ASME J. Mech. Des., **126**(4), pp. 602–608.
[23] Chaudhary, H., and Saha, S. K., 2005, "Matrix Formulation of Constraint Wrenches for Serial Manipulators," *International Conference on Robotics and Automation (ICRA 2005)*, Barcelona, Spain, Apr. 18–22, pp. 4647–4652.
[24] McPhee, J. J., 1996, "On the Use of Linear Graph Theory in Multibody System Dynamics," Nonlinear Dyn., **9**, pp. 73–90.
[25] Shai, O., and Penneck, G. R., 2006, "Extension of Graph Theory to the Duality Between Static Systems and Mechanisms," ASME J. Mech. Des., **128**(1), pp. 179–191.
[26] Muller A., 2004, "Elimination of Redundant Cut Joint Constraints for Multibody System Models," ASME J. Mech. Des., **126**(3), pp. 488–494.
[27] Saha, S. K., and Schiehlen, W. O., 2001, "Recursive Kinematics and Dynamics for Closed Loop Multibody Systems," Mech. Struct. Mach., **29**(2), pp. 143–175.
[28] Angeles, J., and Lee, S., 1988, "The Formulation of Dynamical Equations of Holonomic Mechanical Systems Using a Natural Orthogonal Complement," ASME J. Appl. Mech., **55**(1), pp. 243–244.
[29] Xi, F., 2005, "Tripod Dynamics and Its Inertia Effect," ASME J. Mech. Des., **127**(1), pp. 144–149.
[30] Strang, G., 1998, *Linear Algebra and Its Applications*, Harcourt, Brace, Jovanovich, Orlando.

[31] Shabana, A. A., 1994, *Computational Dynamics*, Wiley, New York.

[32] Khan, W. A., Krovi, V. N., Saha, S. K., and Angeles, J., 2005, "Recursive Kinematics and Inverse Dynamics for a Planar 3R Parallel Manipulator," ASME J. Dyn. Syst., Meas., Control, **127**(4), pp. 529–536.

[33] Chuadhary, H., and Saha, S. K., 2007, "Balancing of Four-Bar Linkages Using Maximum Recursive Dynamic Algorithm," Mech. Mach. Theory, **42**(2), pp. 216–232.

[34] Saha, S. K., Prasad, R., and Mandal, A. K., 2003, "Use of Hoeken's and Pantograph Mechanisms for Carpet Scraping Operations," *Proceedings of the 11th National Conference on Machines and Mechanisms*, IIT, Delhi, Dec. 18–19, pp. 732–738.

[35] MSC.ADAMS (Automated Dynamic Analysis of Mechanical System), Version 2005.0.0, July 22, 2004.

[36] Duffy, J., 1978, "Displacement Analysis of the Generalized RSSR Mechanism," Mech. Mach. Theory, **13**, pp. 533–541.

[37] Bagci, C., 1983, "Complete Balancing of Space Mechanisms-Shaking Force Balancing, ASME Journal of Mechanisms, Transmissions," ASME J. Mech., Transm., Autom. Des., **105**, pp. 609–616.

[38] Angeles, J., 1997, *Fundamental of Robotic Mechanical Systems: Theory, Methods, and Algorithms*, Springer-Verlag, New York.